Eur. Phys. J. D **34**, 183–186 (2005)
DOI: 10.1140/epjd/e2005-00140-7

THE EUROPEAN PHYSICAL JOURNAL D

# Thermodynamic properties of $Au_yAg_x$ bimetallic clusters through the evolutive ensemble

K. Michaelian[a] and I.L. Garzón

Instituto de Física, Universidad Nacional Autónoma de México, A.P. 20-364, 01000 México D.F., México

Received 6 September 2004
Published online 13 July 2005 – 

**Abstract.** The caloric and specific heat curves for the bimetallic nanoclusters $Au_{7-x}Ag_x$ $(x = 0, 3, 4, 7)$ are obtained through a statistical determination of the configurational density of states in the evolutive ensemble obtained with a genetic algorithm. The effect of the value of $x$ (the relative concentrations) on the thermodynamics is studied. Three peaks are observed in the specific heat curves for all values of $x$. This is interpreted as being due to melting, and fragmentation of the cluster into first two, and then into 3 or more parts. A fourth pre-melting peak is observed for $Au_4Ag_3$ and is attributed to a new phenomena related to the breaking of the degeneracy of the permutational isomers. The melting transition for the bimetallic clusters is significantly wider than that for the pure clusters. The boiling transition displays a larger specific heat for the bimetallic clusters.

**PACS.** 36.40.Ei Phase transitions in clusters – 36.40.-c Atomic and molecular clusters

## 1 Introduction

Bimetallic clusters have the potential of adding new flavor to the unique properties of materials at the nano dimension. This even more so than the analogous alloys of the bulk because of the strongly size dependent nature of nanoclusters properties. The investigation of the thermodynamic behavior of clusters is crucial because a correct description of the thermodynamic ensemble leads to a correct ensemble average of the property under consideration. This is particularly important for binary clusters since many, almost degenerate, permutational isomers exist in large numbers, separated by high energy barriers. Compared with pure clusters, the potential energy landscape of binaries is much more complicated and not easily amenable to standard techniques such as molecular dynamics and Monte Carlo.

In this article, we apply a novel ergodic statistical approach to the determination of the thermodynamic properties of bimetallic clusters of $Au_{7-x}Ag_x$ $(x = 0, 3, 4, 7)$, paying particular attention to the effect on the thermodynamics of the non-degenerate permutational isomers.

The $Au_yAg_x$ system has been studied before from the point of view of their structural and electronic properties in the density functional approach [1]. However, to the authors knowledge, there have been no attempts to determine the thermodynamics.

Thermodynamic properties of the bimetallic clusters $Au_xCu_{n-x}$ $(n = 13, 14)$ have been studied by López et al. [2] using a Gupta potential and molecular dynamics simulations. They found that the presence of the low lying permutational isomers does not affect the gross features of the melting-like transition, independently of the concentrations of the components. However, as will be shown below, this is not the case for the $Au_yAg_x$ bimetallic clusters. The discrepancy is most likely due to the difficulty of molecular dynamics remaining ergodic in the complex potential energy landscape of the bimetallics.

## 2 Method

The technique used here and presented in [3,4] is based on an efficient version [5] of the genetic algorithm [6] combined with a conjugate gradient final optimization which can be tuned to find and identify stationary points; minima, saddle points, valleys, etc., all of which influence the thermodynamics. The approach is more efficient and ergodic than traditional approaches because there is no calculation of the forces, Boltzmann weights, nor are Newton's equations of motion solved. Second, there is no problem with potential barriers separating regions of phase space which can cause problems with ergodicity. Third, since evaporation and fragmentation are natural components of the evolutive ensemble, detailed balance can be employed to provide the thermodynamic properties from the solid well into the gas region.

The clusters were modeled with a Gupta many-body potential [7]. The parameters for the homo-interactions were taken from Cleri and Rosato [8] obtained by fitting to the bulk cohesive energy, lattice parameters, and elastic constants, while the hetero-interaction parameters were obtained from a simple arithmetic mean of the parameters

[a] e-mail: karo@fisica.unam.mx

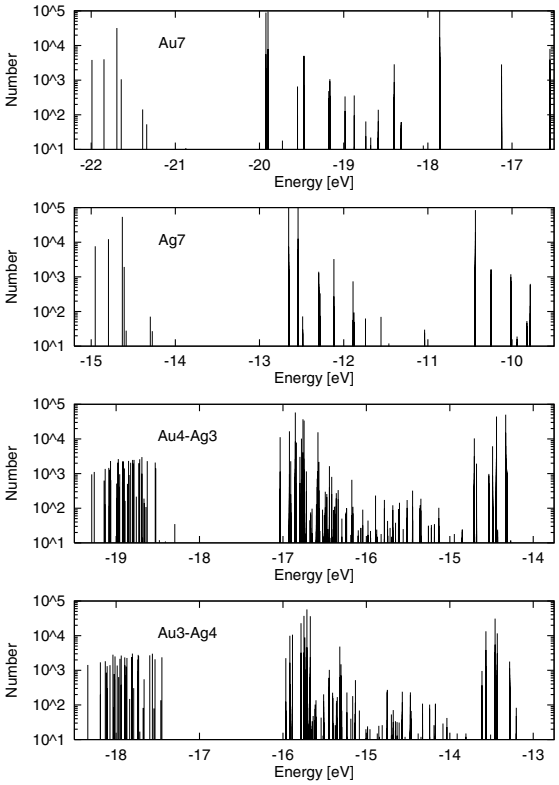


**Fig. 1.** Energy distribution of the stationary points of pure $Au_7$ and $Ag_7$ clusters, and binary $Au_4Ag_3$ and $Au_3Ag_4$ clusters. Their contribution to the evolutive ensemble is given in logarithmic scale on the $y$-axis.

related to the distance, and a geometric mean of the parameters related to the strength.

A very large number of initial configurations generated at random in a fixed volume are globally optimized using the genetic algorithm. When the fitness of the population ceases to change from one generation to the next for 7 consecutive generations, the GA is stopped and the accumulated resulting configurations at this point collectively define the *evolutive ensemble*. It can be shown [3] that this ensemble is similar to a canonical ensemble at an equivalent "temperature", defined principally by the size of the volume in configuration space within which the initial configurations were generated. Each configuration of the evolutive ensemble is locally optimized using the conjugate gradient technique and the resulting stationary point distribution is then used to calculate the total density of states using the superposition approach [9]. From the total density of states, of course, all thermodynamic properties can be determined.

## 3 Energetic and structural results

The energy distribution of the stationary points for the clusters $Au_{7-x}Ag_x$ ($x = 0, 3, 4, 7$) are given in Figure 1. The pure clusters have only four minima with the global minimum for both elements corresponding to the pentagonal bi-pyramid. The four stable isomers are given in Figure 2. In the case of the pure Au clusters, it is known from density functional theory calculations that the global minimum structures are not three dimensional but planar structures [1]. That these are not stable isomers of the potential is a result of the fact that the *s*-*d* electronic shell hybridization due to relativistic effects in Au and giving rise to non-isotropic interactions, cannot be modeled correctly with the isotropic Gupta potential. However, it is emphasized that the main results, concerning the effect of the permutational isomers on the thermodynamics, are relatively independent of the particular form of the isomers.

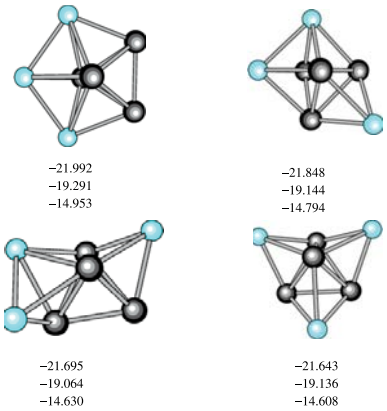


**Fig. 2.** Stable isomers of $Au_7$, $Au_4Ag_3$, and $Ag_7$ with their corresponding energies in eV from top to bottom. In the case of $Au_4Ag_3$ the dark atoms are Au and only the lowest energy premutational isomer of each family is given.

Figure 1 also shows counts corresponding to cluster fragmentation into first two-parts starting at energies of about −19.898 eV for pure Au (a planar trimer plus a 4 atom pyramid) and then fragmentation into three or more parts starting at energies of about −17.859 eV for pure Au (two dimers plus a trimer). Assuming detailed balance, in which the time reversed process is equivalent to the evaporation process, these fragmented configurations correspond to the evaporative part of the evolutive ensemble.

For the case of the binary clusters, with $x = 3, 4$, there are $7!/(4!3!) = 35$ potentially distinct, non-degenerate, permutational isomers for each geometrical minimum of the pure clusters (The possibility exists of completely novel structures but this has not been found for the cases studied here.) This number is an upper limit, the real value depending on the particular symmetries of the configurations. This increase in the density of states and in the width of the energy distribution of the minima for the bimetallic clusters can be clearly observed in Figure 1. The evaporated and fragmented minima also demonstrate a corresponding increase in their number and in the width of their distribution in energy.

The global minimum of the bimetallic clusters is also the pentagonal bi-pyramid. The lowest permutational isomer of each of the geometrical families is given in Figure 2 for $Au_4Ag_3$. Note that the energy ordering of the geometrical isomers of $Au_4Ag_3$ is different from that of the pure Au and pure Ag clusters; the tri-capped tetrahedron (lower right configuration of Fig. 2) is lower in energy than the bi-capped tetrahedron (lower left of Fig. 2). In fact, a careful analysis of the structure of each isomer reveals that for $Au_4Ag_3$ the first and second isomers in energy are from

the pentagonal bi-pyramid family. The third is from the capped prism, the fourth is from the tri-capped tetrahedron family, the fifth and sixth are permutational isomers of the pentagonal bi-pyramid, the seventh and eighth are permutational isomers of the capped prism, while finally the ninth is from the bi-capped tetrahedron family.

The 11 lowest energy isomers of $Au_4Ag_3$ found with the potential were locally optimized using DFT with GGA correction [10]. All isomers of the potential were also stable configurations of the DFT calculations. The energy ordering of the geometrical isomers was the same as that of the potential while there was a difference in the ordering of the permutational isomers at a given geometry. The DFT calculations favored decreased numbers of Au-Au bonds while the potential calculations favored an increase. However, the DFT results are consistent with the potential results in that there is a mixing of the permutational isomers with the geometrical isomers and a spread in their energy distribution. Clearly, this behavior will lead to an important role of the breaking of the degeneracy of the permutational isomers on the thermodynamic behavior.

## 4 Thermodynamic results

We first calculate the total density of states using the superposition principle [9], including minima, important saddle points, and evaporated and fragmented minima. Note that no harmonic supposition has to be made, nor is the symmetry of the stationary point required. Instead, the contribution of each stationary point to the configurational density of states is determined statistically [3].

The total density of states at an energy $E$ is

$$\Omega(E) = \int_{V_0}^{E} \Omega_C(V)\Omega_K(E-V)dV, \tag{1}$$

where the integration is from the energy of the global minimum $V_0$ up to energy $E$. The kinetic density of states can be shown to be [11]

$$\Omega_K(E-V) = B(E-V)^{\nu/2-1}, \tag{2}$$

where $B$ is a constant and $\nu$ is the total number of degrees of freedom of the system ($3N-6$ for comparing results with the molecular dynamics ensemble).

The configurational density of states $\Omega_C(V)$ can be determined from the stationary point distributions $\{S_i, \mathcal{N}_i\}$ (Fig. 1) where $S_i$ is the energy of the stationary point and the $\mathcal{N}_i$ is the number of times the point was found. It can be shown that the evolutive ensemble is similar to the canonical ensemble at a given temperature $T_0$, giving a Maxwell-like distribution of the potential energies of the configurations [3]. $T_0$ is found to be proportional to the volume used to generate the initial configurations and inversely proportional to both the population size and the number of generations specified to converge the GA.

The configurational density of states is then

$$\Omega_C(S_i) = \mathcal{N}_i \exp(S_i/k_BT_0). \tag{3}$$

For the discrete stationary point distribution $\{S_i, \mathcal{N}_i\}$, equation (1) becomes

$$\Omega(E_l) = \sum_{i=1}^{l} \mathcal{N}_i \exp(S_i/k_BT_0)(E_l - S_i)^{\nu/2-1}, \tag{4}$$

where the sum is up to the highest stationary point $S_l$ accessible at $E_l$ ($S_l < E_l$) and we have left out an unimportant multiplicative constant.

From the entropy in terms of the density of states

$$\mathcal{S}(E) = k_B \ln(\Omega(E)) \tag{5}$$

the *thermodynamic* temperature can be determined as

$$T_T(E) \equiv (\partial\mathcal{S}/\partial E)^{-1}. \tag{6}$$

Defining

$$F_0(E,T_0) = \sum_i \mathcal{N}_i \exp(S_i/k_BT_0)(E-S_i)^{\nu/2},$$
$$F_1(E,T_0) = \sum_i \mathcal{N}_i \exp(S_i/k_BT_0)(E-S_i)^{\nu/2-1},$$
$$F_2(E,T_0) = \sum_i \mathcal{N}_i \exp(S_i/k_BT_0)(E-S_i)^{\nu/2-2}$$

gives

$$T_T(E) = (1/k_B(\nu-1))(F_1/F_2). \tag{7}$$

The *kinetic* temperature, which can be used for comparing with molecular dynamics results, is

$$T_K(E) = (1/k_B\nu)(F_0/F_1) \tag{8}$$

and the specific heat

$$C_v(E) \equiv \frac{1}{k_BN}\left(\frac{\partial T_K(E)}{\partial E}\right)^{-1} \tag{9}$$

giving

$$C_v(E) = \frac{\nu}{N}\left[\frac{\nu}{2} - \left(\frac{\nu}{2}-1\right)\frac{F_0F_2}{F_1^2}\right]^{-1}. \tag{10}$$

The microcanonical caloric and specific heat curves using the kinetic temperature obtained in this manner for $Au_{7-x}Ag_x$ with $\nu = 3N-6$ are given in Figures 3 and 4. Figure 3 focuses on just the melting transition region of the full caloric and specific heat curves given in Figure 4. Note that the melting transition is wider for the binary clusters than for either of the two pure clusters. This is a result of an increase in the width of the minima distribution due to breaking the degeneracy of the permutational isomers (Fig. 1). Second, the $Au_4Ag_3$ specific heat curve shows a small pre-melting peak. Its origin can be ascribed to a completely new phenomena, breaking of the degeneracy of the global minimum and thus the introduction of a second permutational isomer of the global minimum of slightly higher energy (also the case for the DFT calculations) and with a slightly larger attraction basin (see Fig. 1). This now non-degenerate isomer plays a similar

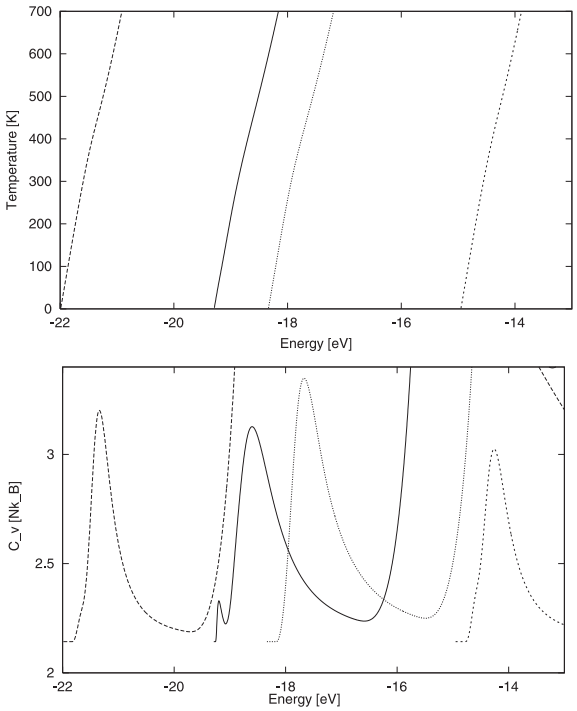


**Fig. 3.** Caloric and specific heat curves calculated through the statistical model in the microcanonical ensemble using the stationary point distribution for pure Au – long dashed curve, for pure Ag – short dashed curve, for $Au_4Ag_3$ – solid curve, and $Au_3Ag_4$ – points. The peaks in the specific heat curve correspond to the melting transition.

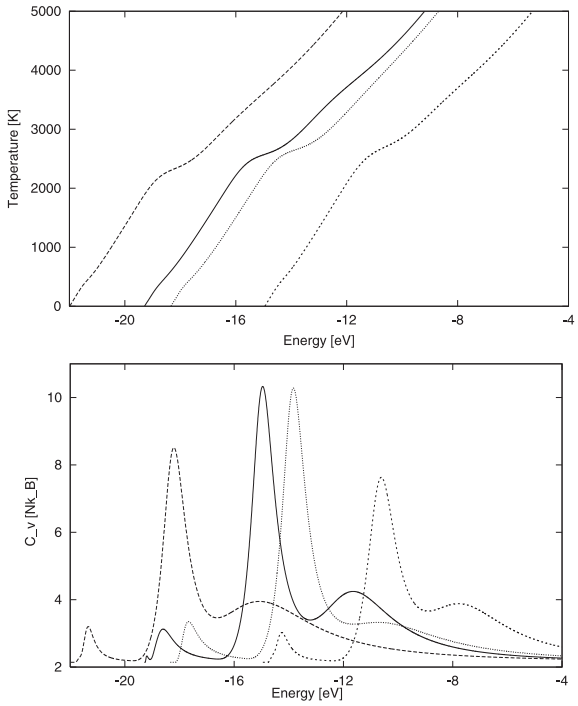


**Fig. 4.** Same as for Figure 3 but on a larger energy scale in which the fragmentation peaks can be seen in the specific heat curves.

role to that of the slightly higher energy isomers visited by a single atom outside a closed shell in the normal pre-melting found, for example in pure clusters of 14 atoms.

The second peak in the specific heat curves given in Figure 4 is due to the two-fold fragmentation and is significantly higher for the binary clusters than for the pure clusters. This is due to a relative broadening of the fragment energy spectrum due to breaking the degeneracy of the fragments (see Fig. 1). The third, 3-fold fragmentation peak in the specific heat curve for $Au_4Ag_3$ also shows an enhancement with respect to that of the pure clusters. This is not the case for $Au_3Ag_4$, however, which in fact shows a de-enhancement.

Finally, there is also a small increase in the boiling temperature for the binary clusters over the pure Au clusters, giving both of them boiling temperatures closer to that of Ag than to Au.

## 5 Conclusions

We have studied the thermodynamics of bimetallic clusters using a novel ergodic statistical approach employing a Gupta potential and confirming the isomer energy distributions using DFT calculations. In contrast to the results obtained in [2] for Au-Cu clusters, we find that the thermodynamics of the bimetallic Au-Ag clusters is significantly different than that of the pure clusters. First, their melting transition is wider. Second, pre-melting may occur due to the breaking of the degeneracy and the subsequent introduction of a permutational isomer of the global minimum at only slightly higher energy. Third, the specific heats are greater at the boiling transition. Fourth, the relative sizes of the fragmentation peaks in the specific heat may be significantly different, depending on the energetics of the degeneracy breaking of the permutational isomers. These findings required a truly ergodic technique such as the one presented here for their elucidation.

The financial support of DGAPA-UNAM project 104402 and CONACyT grant 40393-A is appreciated.

## References

1. V. Bonačić-Koutecký, J. Burda, R. Mitrić, M. Ge, G. Zampella, P. Fantucci, J. Chem. Phys. **117**, 3120 (2002)
2. M.J. López, P.A. Marcos, J.A. Alonso, J. Chem. Phys. **104**, 1056 (1996)
3. K. Michaelian, A. Reyes-Nava, A. Támez, I.L. Garzón, to be published
4. K. Michaelian, A. Taméz, I.L. Garzón, Chem. Phys. Lett. **370**, 654 (2003)
5. K. Michaelian, Chem. Phys. Lett. **293**, 202 (1998)
6. K. Michaelian, Am. J. Phys. **66**, 231 (1998)
7. R.P. Gupta, Phys. Rev. B **23**, 6265 (1981)
8. F. Cleri, V. Rostato, Phys. Rev. B **48**, 22 (1993)
9. D.J. Wales, Mol. Phys. **78**, 151 (1993)
10. D. Sánchez-Portal, P. Ordejón, E. Artacho, J.M. Soler, Int. J. Quantum Chem. **65**, 453 (1997)
11. E.M. Pearson, T. Halicioglu, W.A. Tiller, Phys. Rev. A **32**, 3030 (1985)